

Supplemental Materials

Molecular Biology of the Cell

Imai et al.

Supplemental Information for

Density imaging of heterochromatin in live cells using orientation-independent-DIC microscopy

Ryosuke Imai, Tadasu Nozaki, Tomomi Tani, Kazunari Kaizu, Kayo Hibino, Satoru Ide, Sachiko Tamura, Koichi Takahashi, Michael Shribak*, and Kazuhiro Maeshima*

This file includes:

Supplemental Procedure (Mathematical model of OI-DIC microscopy)

Supplemental Figures S1-S7

Caption for Movie S1

Supplemental References

Other Supplemental Materials for this manuscript include the following:

Supplemental Movie S1

Supplemental Procedure

Mathematical model of OI-DIC microscopy

For convenience of the reader we briefly explain the mathematical principles of OI-DIC technique and one of image processing algorithms. The OI-DIC mathematical model along with several processing algorithms were reported in detail elsewhere (Shribak and Inoue, 2006; Shribak, 2013; Shribak *et al.*, 2017).

The intensity distribution in the DIC image $I(x,y)$ can be described by using a model of interference of two overlapping identical coherent images with optical path difference $OPD(x,y)$, slightly offset from each other:

$$I(x,y) = \tilde{I} \sin^2 \left\{ \frac{\pi}{\lambda} [\Gamma + \mathbf{d} \cdot \mathbf{G}(x,y)] \right\} + I_c(x,y),$$

where \tilde{I} is the initial beam intensity, λ is wavelength, Γ is bias, \mathbf{d} is shear vector, $\mathbf{G}(x,y)$ is the optical path difference gradient vector, and $I_c(x,y)$ corresponds to an offset of the intensity signal, which caused by the stray light.

The optical path difference gradient vector $\mathbf{G}(x,y)$ is the following:

$$\mathbf{G}(x,y) = \left(\frac{d(OPD(x,y))}{dx}, \frac{d(OPD(x,y))}{dy} \right) = (\gamma(x,y) \cos \theta(x,y), \gamma(x,y) \sin \theta(x,y)),$$

where $\gamma(x,y)$ and $\theta(x,y)$ are optical path difference gradient magnitude and azimuth, respectively.

In order to map the optical path difference gradient vector $\mathbf{G}(x,y)$ the OI-DIC microscope varies shear vector \mathbf{d} and bias Γ . We capture two sets of raw DIC images at shear directions -45° and $+45^\circ$ with negative, zero and positive biases: $-\Gamma_0$, 0 , and $+\Gamma_0$. Typically we use biases $\pm 0.15\lambda$ and 0 .

The following group of equations represents these six DIC images:

$$I_{i,j}(x,y) = \tilde{I} \sin^2 \left\{ \frac{\pi}{\lambda} \left[j\Gamma_0 + \sqrt{2} d \gamma(x,y) \cos \left(\theta(x,y) - (-1)^i \frac{\pi}{4} \right) \right] \right\} + I_c(x,y),$$

where $j = -1, 0, 1$, and d is shear amount (magnitude of shear vector).

Initially two terms are computed ($i = 1, 2$):

$$A_i(x,y) = \frac{I_{i,1}(x,y) - I_{i,-1}(x,y)}{I_{i,1}(x,y) + I_{i,-1}(x,y) - 2I_{i,0}(x,y)} \tan \left(\frac{\pi \Gamma_0}{\lambda} \right)$$

Using the obtained terms we can calculate the quantitative two-dimension distributions of the gradient magnitude and azimuth of optical path difference in the specimen as:

$$\gamma(x,y) = \frac{\lambda}{2\sqrt{2}\pi d} \sqrt{\sum_{i=1}^2 \arctan^2[A_i(x,y)]}$$

$$\theta(x,y) = \arctan\left(\frac{\arctan A_2(x,y)}{\arctan A_1(x,y)}\right) - \frac{\pi}{4}$$

The gradient magnitude represents increment of the optical path difference, which is in nanometers, along lateral coordinate, which is also in nanometers. Thus, the gradient magnitude is unitless.

The obtained two-dimension distribution of optical path difference gradient vector $\mathbf{G}(x,y)$ is used for computing the optical path difference map $OPD(x,y)$. For this purpose the gradient vector $\mathbf{G}(x,y)$ can be presented as a complex number:

$$\mathbf{G}(x,y) = \frac{\partial(OPD(x,y))}{\partial x} + i \frac{\partial\phi(OPD(x,y))}{\partial y} = \gamma(x,y)e^{i\theta(x,y)}, \quad (1)$$

where real and imaginary parts are X- and Y- components of the gradient vector, respectively.

At first we apply the 2-dimensional Fourier transform to the left and the middle parts of the equation above. Then the resultant integral equation can be solved by partial integration. After using the inverse 2-dimensional Fourier transform we receive the following formula for computation of the optical path difference $OPD(x,y)$:

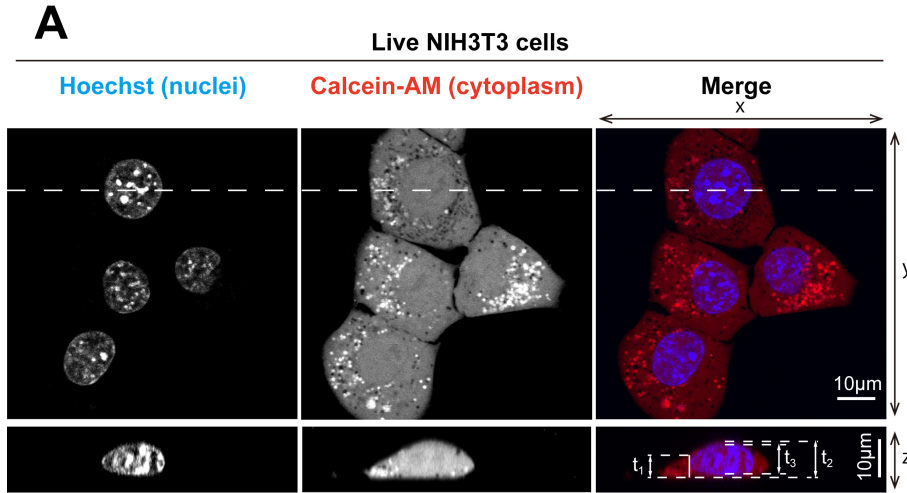
$$OPD(x,y) = F^{-1} \left[\frac{F[\mathbf{G}(x,y)]}{i(\omega_x + i\omega_y)} \right],$$

where ω_x and ω_y are spatial angular frequencies.

Taking into account the right part of equation (1), finally we get formula for computing the OPD:

$$OPD(x,y) = F^{-1} \left[\frac{F[\gamma(x,y)e^{i\theta(x,y)}]}{i(\omega_x + i\omega_y)} \right].$$

Then a computed two-dimensional distribution of the optical path difference is transformed into quantitative 8-bit grayscale image (map), where the image brightness is linearly proportional to value of the OPD and the maximum grey level of 255 corresponds to the chosen OPD ceiling.



B Thickness of each point (Median \pm quartile deviation)

	t_1	t_2	t_3	
Live NIH3T3	6.35 \pm 0.69	8.21 \pm 0.93	6.90 \pm 0.59	(n = 21)
NIH3T3 MeOH fixed	* 5.65	* 7.31	6.14 \pm 0.87	(n = 28)
NIH3T3 FA fixed	* 4.54	* 5.87	4.94 \pm 0.48	(n = 26)
Live RPE1	* 4.54	* 5.87	4.94 \pm 0.62	(n = 20)

* Calculated from ratio of t_1 : t_2 : t_3 of NIH3T3 untreated live cells

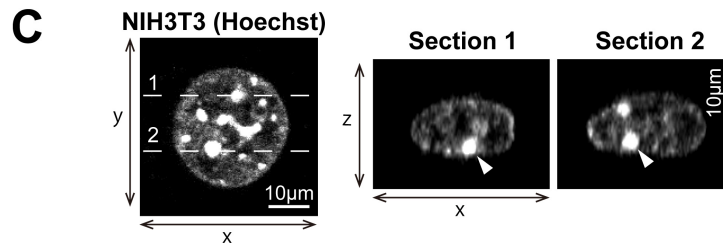


Figure S1

Supplemental Figure S1

(A) Thickness measurements of nuclei and cytoplasm. DNA and cytoplasm were stained with Hoechst 33342 and Calcein-AM, respectively. x-y images (upper) and cross-sectional (x-z) images (lower) along the dashed white lines are shown. To calculate RI, three thickness measurements were taken: t_1 , cytoplasm region adjacent to the nucleus; t_2 , the thickest region of a cell, including the cytoplasm and nucleus; t_3 , the thickest region of a nucleus. (B) Table of the measured thicknesses (t_1 , t_2 , and t_3) for each cell line and condition. The values are presented as median \pm quartile deviation. (C) Cross-sectional views (center and right) of pericentric heterochromatin foci along two dashed white lines indicated in the x-y image (left). Note that the pericentric foci (arrowheads) seem to be spherical.

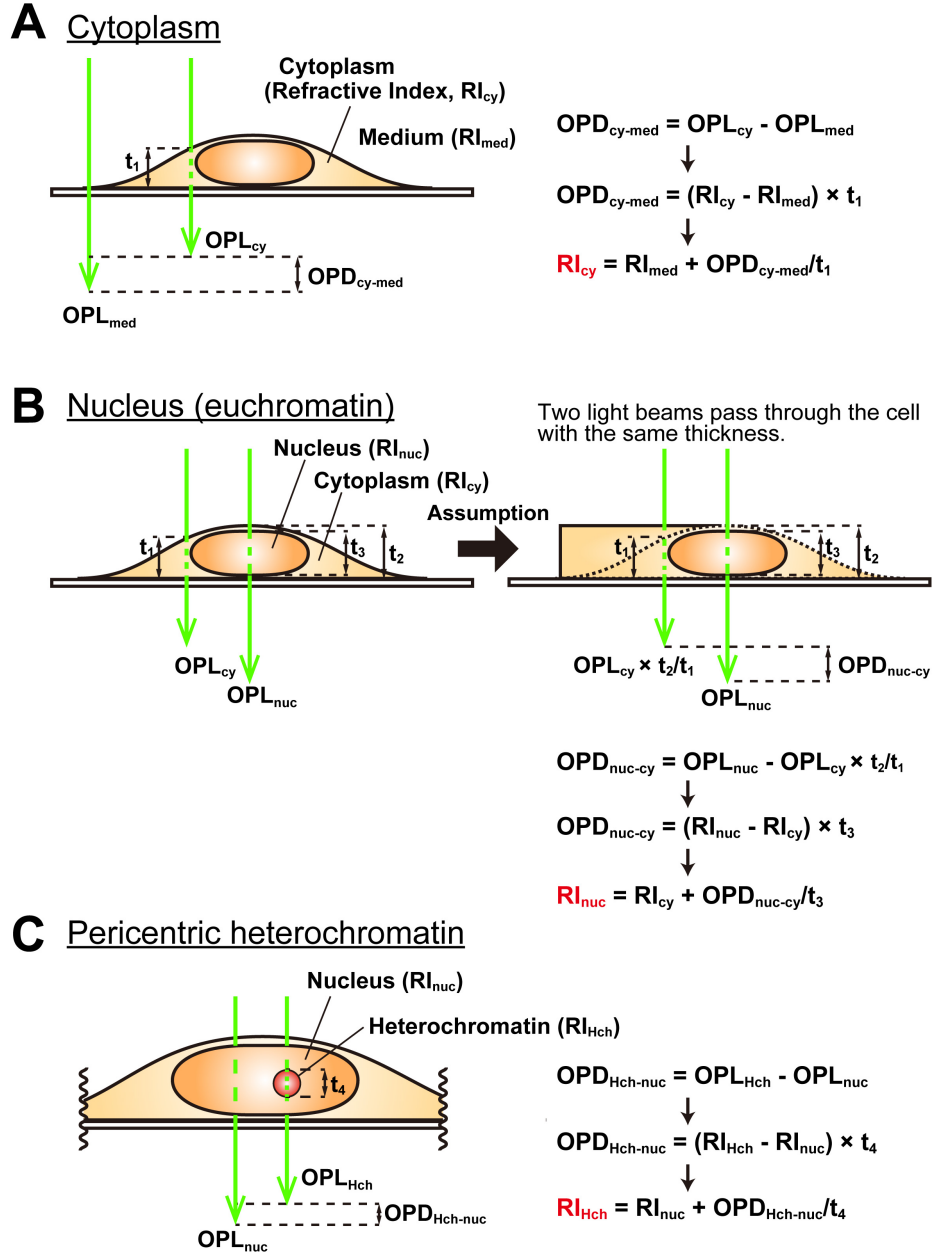


Figure S2

Supplemental Figure S2

(A) A calculation scheme for the RI_{cy} . We obtained RI_{cy} based on the measured values for OPD_{cy-med} , thickness t_1 and RI_{med} . (B) RI_{nuc} (euchromatin). Because the thicknesses of the sample through each of the two polarized beam passed should be the same, we multiplied OPD_{cy} by t_2/t_1 to obtain OPD_{nuc-cy} (t_2 , thickest point of the cell including nucleus and cytoplasm; t_1 , thickness of cytoplasm region beside nucleus) (see also Supplemental Figure S1). RI_{nuc} was calculated based on RI_{cy} and nuclear thickness t_3 . (C) Heterochromatin foci RI (RI_{Hch}). The heterochromatin focus thickness t_4 was assumed to be their width (see also Supplemental Figure S1).

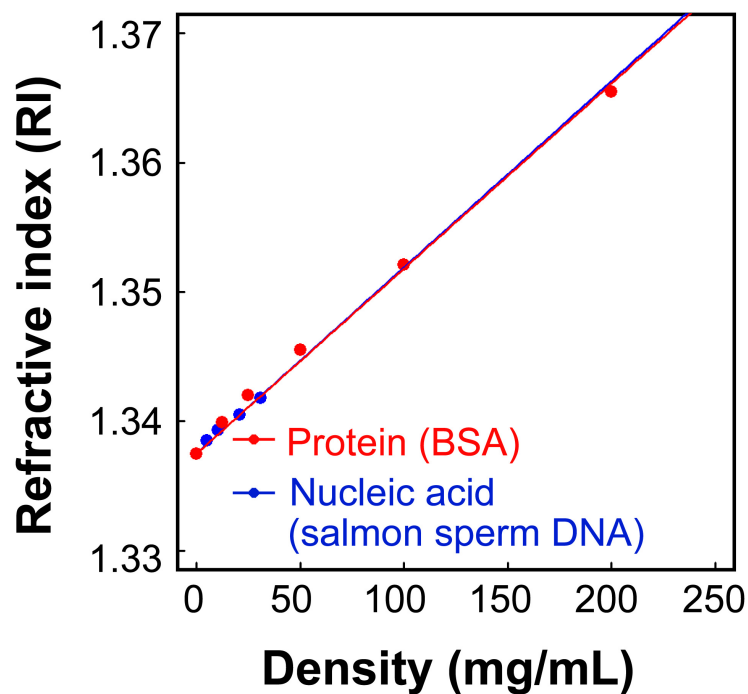


Figure S3

Supplemental Figure S3

The calibration curve of RIs versus the density of standard solutions for protein or nucleic acid. For details, see the Materials and Methods section. $RI = 1.3375 + 1.4 \times 10^{-4} (\text{mL/mg}) \times C$ (RI, the refractive index; C, the concentration of the nucleic acids or proteins [mg/mL]).

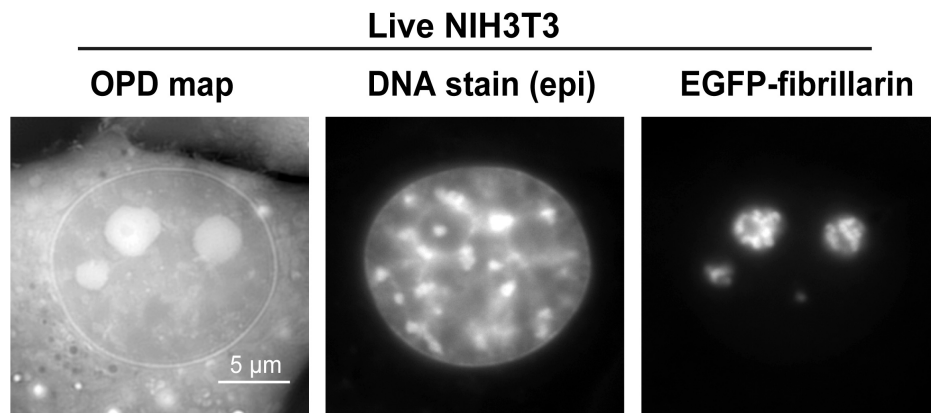


Figure S4

Supplemental Figure S4

OPD maps (left), DNA staining (center) and EGFP-fibrillarin (right) images of live NIH3T3 cells. The high-density regions in OPD maps (which co-localized with EGFP-fibrillarin signals, a nucleoli marker) were nucleoli.

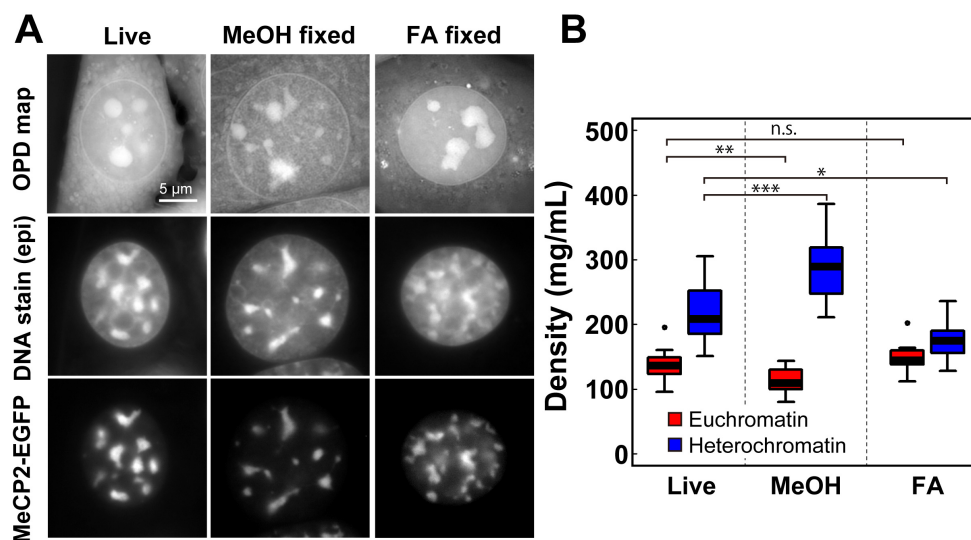


Figure S5

Supplemental Figure S5

Density changes in cells upon fixation. **(A)** OPD maps (1st row), DNA staining (2nd row) and MeCP2-EGFP (3rd row) images of live NIH3T3 cells with MeOH fixation (center column) and FA fixation (right column). **(B)** The densities of euchromatin and pericentric heterochromatin in MeOH- and FA-fixed cells. Under the MeOH fixation condition, $n = 10$ for euchromatin and $n = 20$ for heterochromatin. Under the FA fixation condition, $n = 8$ for euchromatin and $n = 16$ for heterochromatin. n.s., not significant; * $p < 0.01$; ** $p < 0.001$; *** $p < 0.0001$, Student's t -test.

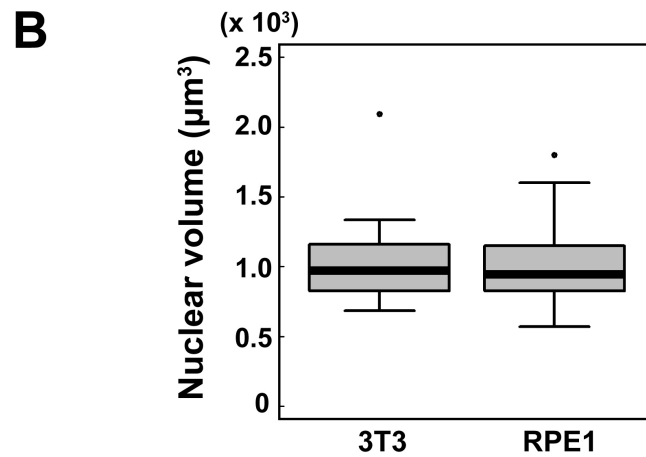
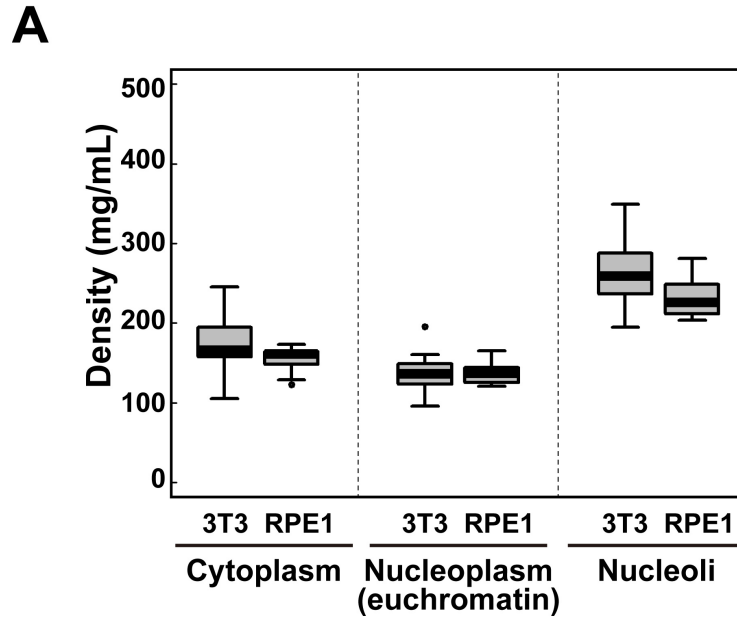


Figure S6

Supplemental Figure S6

(A) The densities of cytoplasm, nucleoplasm (euchromatin), and nucleoli in NIH3T3 and RPE1 cells. 3T3, n = 13 cells; RPE1, n = 10 cells. (B) Nuclear volume measurements of the two cell lines. NIH3T3, n = 25 cells; RPE1, n = 23 cells

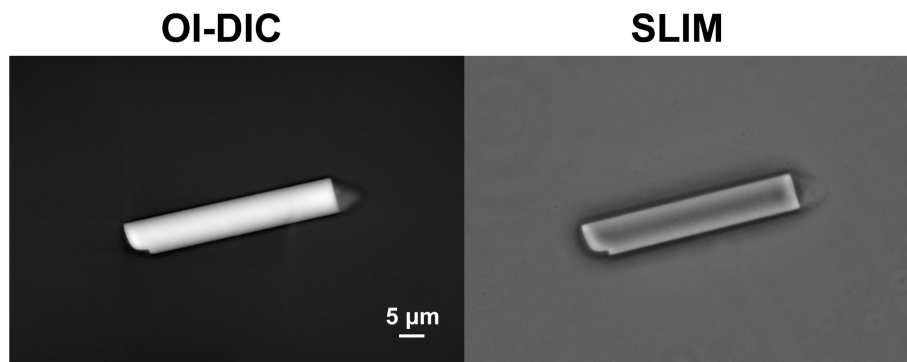


Figure S7

Supplemental Figure S7

OPD images of 7- μm -diameter glass rod, taken with the OI-DIC (left) and Spatial Light Interference Microscopy (SLIM) (right). The OI-DIC depicts the expected image. The SLIM image displays artifacts: a strong shadow-in in the rod center and a halo around the rod.

Supplemental Movie 1

A typical result of diffusion simulation in the left (136 mg/mL) and right (208 mg/mL) halves, corresponding to the *in vivo* euchromatin and heterochromatin environments, respectively.

Transparent blue spheres are crowding agents (nucleosomes and non-nucleosomal materials), and red spheres are tracers. The coordinates of the spheres were recorded at 1 μ s/frame for 3 ms (3,000 frames). To aid in visualization, only part of the simulation space is presented (20% of the entire space, 210 \times 210 \times 42 nm).

Supplemental References

Shribak, M. (2013). Quantitative orientation-independent differential interference contrast microscope with fast switching shear direction and bias modulation. *J Opt Soc Am A Opt Image Sci Vis* 30, 769-782.

Shribak, M., and Inoue, S. (2006). Orientation-independent differential interference contrast microscopy. *Appl Opt* 45, 460-469.

Shribak, M., Larkin, K.G., and Biggs, D. (2017). Mapping optical path length and image enhancement using quantitative orientation-independent differential interference contrast microscopy. *J Biomed Opt* 22, 16006.